Generalized Chaplygin gas model, supernovae, and cosmic topology

M. C. Bento,[1,*] O. Bertolami,[1,†] M. J. Rebouças,[2,‡] and P. T. Silva[1,§]

[1]*Departamento de Física, Instituto Superior Técnico, Avenida Rovisco Pais, 1049-001 Lisboa, Portugal*
[2]*Centro Brasileiro de Pesquisas Físicas, Rua Dr. Xavier Sigaud 150, 22290-180 Rio de Janeiro—RJ, Brazil*

In this work we study to which extent the knowledge of spatial topology may place constraints on the parameters of the generalized Chaplygin gas (GCG) model for unification of dark energy and dark matter. By using both the Poincaré dodecahedral and binary octahedral spaces as the observable spatial topologies, we examine the current type Ia supernovae (SNe Ia) constraints on the GCG model parameters. We show that the knowledge of spatial topology does provide additional constraints on the A_s parameter of the GCG model but does not lift the degeneracy of the α parameter.

I. INTRODUCTION

Recently, the generalized Chaplygin gas (GCG) model [1–3] has attracted considerable attention given its potential to account for the observed accelerated expansion of the Universe [4], and to describe in a simple scheme, both the negative pressure dark energy component as well as the pressureless dark matter component. In terms of the critical density, the contribution of each component is about two thirds for dark energy and one third for dark matter [5].

In the GCG proposal, the dark components are described through a perfect fluid of density ρ_{ch} and pressure p_{ch} with an exotic equation of state

$$p_{ch} = -\frac{A}{\rho_{ch}^\alpha}, \tag{1}$$

where A and α are positive constants. For $\alpha = 1$, the equation of state is reduced to the Chaplygin gas scenario [1]. The striking feature of this model is that it allows for an unification of dark energy and dark matter [2,3].

The parameters of the GCG or indeed any dark energy model are known to be affected by the spatial geometry the Universe. Physicists describe the Universe as a manifold, which is characterized by its geometry and its topology. Two fundamental questions regarding the nature of the Universe concern the geometry and topology of the 3-dimensional space. Geometry is a local feature related with the intrinsic curvature of the 3-dimensional space and can be tested by studies of the cosmic microwave background radiation (CMBR) such as the Wilkinson Microwave Anisotropy Probe (WMAP). Topology is a global property that characterizes its shape and size. Geometry constrains but does not fix the topology of the spatial sections. In a locally spatially homogeneous and isotropic universe the topology of its spatial section dictates its geometry. Within the framework of the standard Friedmann–Lemaître–Robertson–Walker (FLRW) cosmology, the universe is modeled by a space-time manifold $\mathcal{M}_4$ which is decomposed into $\mathcal{M}_4 = \mathbb{R} \times M_3$ and endowed with a locally (spatially) homogeneous and isotropic metric

$$ds^2 = -dt^2 + a^2(t)[d\chi^2 + f^2(\chi)(d\theta^2 + \sin^2\theta d\phi^2)], \tag{2}$$

where $f(\chi) = (\chi, \sin\chi, \text{or } \sinh\chi)$ depending on the sign of the constant spatial curvature ($k = 0, 1, -1$).

The 3-dimensional space where we live in is usually taken to be one of the following simply-connected spaces: Euclidean $\mathbb{R}^3$, spherical $\mathbb{S}^3$, or hyperbolic space $\mathbb{H}^3$. However, given that the connectedness of the spatial sections M_3 has not been determined by cosmological observations, and since geometry does not fix the topology, our 3-dimensional space may equally well be one of the possible multiply-connected quotient manifolds $M_3 = \tilde{M}/\Gamma$, where Γ is a fixed-point-free group of isometries of the covering space $\tilde{M} = (\mathbb{R}^3, \mathbb{S}^3, \mathbb{H}^3)$.

Thus, for instance, for the Euclidean geometry ($k = 0$) besides $\mathbb{R}^3$ there are 10 classes of topologically distinct compact 3-spaces consistent with this geometry, while for both the spherical ($k = 1$) and hyperbolic ($k = -1$) geometries there are an infinite number of topologically inequivalent compact manifolds with nontrivial topology that admit these geometries.

Recently, different strategies and methods to probe a nontrivial topology of the spatial sections of the Universe have been devised (see, e.g., the review articles Refs. [6] and also Refs. [7] for details on cosmic crystallographic methods). An immediate observational consequence of a detectable nontrivial topology[1] of the 3-dimensional space M_3 is that the sky will exhibit multiple (topological) images of either cosmic objects or specific spots on the

---

*Electronic address: bento@sirius.ist.utl.pt
Also at CFTP, Instituto Superior Técnico, Av. Rovisco Pais, 1049-001 Lisboa
†Electronic address: orfeu@cosmos.ist.utl.pt
‡Electronic address: reboucas@cbpf.br
§Electronic address: paptms@ist.utl.pt

---

[1]The extent to which a nontrivial topology may be detected was discussed in Refs. [8].

CMBR. The so-called "circles-in-the-sky" method, for example, relies on multiple images of correlated circles in the CMBR maps [9]. In a space with a detectable non-trivial topology, the sphere of last scattering intersects some of its topological images along pairs of circles of equal radii, centered at different points on the last scattering sphere (LSS), with the same distribution of temperature fluctuations, δT. Since the mapping from the last scattering surface to the night sky sphere preserves circles [10], these pairs of matching circles will be imprinted on the CMBR anisotropy sky maps regardless of the background geometry or detectable topology. As a consequence, to observationally probe a nontrivial topology one should scrutinize the full-sky CMBR maps in order to extract the correlated circles, whose angular radii and relative position of their centers can be used to determine the topology of the Universe. In this way, a nontrivial topology of the space section of the Universe is observable, and can be probed for all locally homogeneous and isotropic geometries.

In this regard, in a recent work [11] in the context of the ΛCDM model, the Poincaré dodecahedral space was used as the observable spatial topology of the Universe to reanalyze the current type Ia supernovae (SNe Ia) constraints on the density parameters associated with dark matter (Ω_m) and dark energy (Ω_Λ). As a result, it has been shown that the knowledge of the Poincaré dodecahedral space topology through the "circles-in-the-sky" method gives rise to stringent constraints on the energy density parameters allowed by the conventional SNe Ia observations, reducing considerably the inherent degeneracies of the current measurements. Given this encouraging result it is natural to assess to what extent this method can be useful for determining the parameters of more complex dark energy models. In this paper, we address these questions by focusing on the constraints that cosmic topology[2] together with current SNe Ia data pose on the parameters of the GCG model. To this end, we use the Poincaré dodecahedral and the binary octahedral spaces as the topologies of the spatial sections of the Universe[3] to reanalyze current constraints on the parameters of the GCG model, as provided by the so-called *gold* sample of 157 SNe Ia [16].

II. THE GENERALIZED CHAPLYGIN GAS MODEL

The integration of the energy conservation equation with the equation of state (1), yields [3]

$$\rho_{ch} = \rho_{ch0}\left[A_s + \frac{(1 - A_s)}{a^{3(1+\alpha)}}\right]^{1/(1+\alpha)}, \qquad (3)$$

where ρ_{ch0} is the present energy density of the GCG and $A_s \equiv A/\rho_{ch0}^{(1+\alpha)}$. One of the most striking features of this expression is that the energy density, ρ_{ch}, interpolates between a dust dominated phase, $\rho_{ch} \propto a^{-3}$, in the past and a de-Sitter phase, $\rho_{ch} = -p_{ch}$, at late times. This property makes the GCG model an interesting candidate for the unification of dark matter and dark energy. Moreover, one can see from the above equation that A_s must lie in the range $0 \leq A_s \leq 1$: for $A_s = 0$, GCG behaves always as matter whereas for $A_s = 1$, it behaves always as a cosmological constant. We should point out, however, that if one aims to unify dark matter and dark energy, one has to exclude these two possibilities resulting in the range $0 < A_s < 1$. The value $\alpha = 0$ corresponds to the ΛCDM model. Notice that in most phenomenological studies, the range $0 \leq \alpha \leq 1$ is considered, however it is shown that the most recent supernovae data favors $\alpha > 1$ values [17,18].

Friedmann's equation for a nonflat unified GCG model is given by [19]

$$\left(\frac{H}{H_0}\right)^2 = \Omega_{r0}(1 + z)^4 + \Omega_{b0}(1 + z)^3 + \Omega_k(1 + z)^2$$
$$+ \Omega_{\text{dark}}[A_s + (1 - A_s)(1 + z)^{3(1+\alpha)}]^{1/(1+\alpha)}. \qquad (4)$$

where $\Omega_{\text{dark}} = 1 - \Omega_k - \Omega_{b0} - \Omega_{r0}$, $\Omega_k = 1 - \Omega_{\text{tot}}$ and $\Omega_{b0} = 0.04$, $\Omega_{r0} = 9.89 \times 10^{-5}$ are the baryon and radiation energy density contributions at present. This model has been thoroughly scrutinized from the observational point of view; indeed, its compatibility with the CMBR peak location and amplitudes [19,20], with SNe Ia data [17,18,21], gravitational lensing statistics [22,23] and gamma-ray bursts [24] has been extensively examined.

III. COSMIC TOPOLOGY ANALYSIS

The observed values of the power measured by WMAP of the CMBR quadrupole ($\ell = 2$) and octopole ($\ell = 3$) moments, and of the total density $\Omega_{\text{tot}} = 1.02 \pm 0.02$ reported by WMAP team [15] have motivated the suggestion of the Poincaré dodecahedral space topology as an explanation for the observed low power of $\ell = 2$ and $\ell = 3$ multipoles [12]. Since then the dodecahedral space has been the scope of various studies [13,25–27], where some important features have been considered. As a consequence, it turns out that a universe with the Poincaré dodecahedral space section squares with WMAP data in that it accounts for the suppression of power at large scales observed by WMAP, and fits the WMAP temperature two-point correlation function [13,14], retaining the standard FLRW description for local physics.

In a recent paper, Aurich *et al.* [14] have examined the behavior of both the CMBR angular power spectrum and the two-point temperature correlation function for typical groups Γ for which the spatial section $\mathbb{S}^3/\Gamma$ is (globally)

---

[2]In line with current literature, by topology of the Universe we mean the topology of the spatial section M_3.

[3]These spatial topologies account for the low value of the CMBR quadrupole and octopole moments measured by the WMAP team, and fit the temperature two-point correlation function, for values of the total density within the reported range [12–15].

homogeneous. They have found that only three out of infinitely many manifolds fit WMAP's low multipole ($\ell \leq 30$) power spectrum the temperature correlations function, namely, the Poincaré dodecahedron $\mathcal{D} = \mathbb{S}^3/I^*$, $\mathcal{O} = \mathbb{S}^3/O^*$ and $\mathcal{T} = \mathbb{S}^3/T^*$. Here I^*, O^*, and T^* denotes, respectively, the binary icosahedral group, the binary octahedral group, and the binary tetrahedral group[4] (for more details on the globally homogeneous spherical manifold see the Appendix).

Furthermore, the authors of Ref. [14] find that if Ω_{tot} is restricted to the interval [1.00, 1.04], the space $\mathcal{T}$ is excluded since it requires a value of Ω_{tot} in the range [1.06, 1.07]. Thus, they conclude that there remain only two globally homogeneous spherical spaces that account for WMAP observed power spectrum, and fits the WMAP temperature two-point correlation function, namely $\mathcal{D}$ and $\mathcal{O}$. In this paper, we shall restrict ourselves to the study of the FLRW model with $\mathcal{D}$ and $\mathcal{O}$ sections. We begin by recalling that in the range of Ω_{tot} where they fit the WMAP data, these manifolds predict pairs of antipodal matched circles in the LSS. Figure 1 gives an illustration of two of these antipodal circles.

The distance between the centers of each pair of circles is twice the radius r_{inj} of the smallest sphere inscribable in the fundamental cells of these manifolds. A straightforward use of a Napier's rule on the right-angled spherical triangle shown in Fig. 1 gives a relation between the angular radius γ and the angular sides r_{inj} and radius χ_{lss} of the last scattering sphere, namely

$$\cos\gamma = \frac{\tan r_{inj}}{\tan\chi_{lss}}, \qquad (5)$$

where r_{inj} is a topological invariant, equal to $\pi/10$ and $\pi/8$ for, respectively, $\mathcal{D}$ and $\mathcal{O}$. This equation can be solved for χ_{lss} to give

$$\chi_{lss} = \tan^{-1}\left[\frac{\tan r_{inj}}{\cos\gamma}\right], \qquad (6)$$

where the distance χ_{lss} to the origin *in units of the curvature radius*, $a_0 = a(t_0) = (H_0\sqrt{|1 - \Omega_{\text{tot}}|})^{-1}$, is given by

$$\chi_{lss} = \frac{d_{lss}}{a_0} = \sqrt{|\Omega_k|} \int_1^{1+z_{lss}} \frac{H_0}{H(x)} dx, \qquad (7)$$

---

[4]A preliminary search failed to find the antipodal matched circles in the WMAP sky maps predicted by the Poincaré model [25]. In a second search for these circles only a nonconclusive indication for the correlated circles has been reported for $\mathcal{D}$ and $\mathcal{T}$ spaces [28]. Notice, however, that the Doppler and integrated Sachs-Wolfe contributions may be strong enough to blur the circles, and thus the correlated circles can be overlooked in the CMB sky maps search [13]. In this way, the "absence of evidence may not be evidence of absence", specially given that effects such as Sunyaev-Zeldovich, lensing and the finite thickness of the LSS, as well as possible systematics in the removal of the foregrounds, can further damage the topological circle matching.
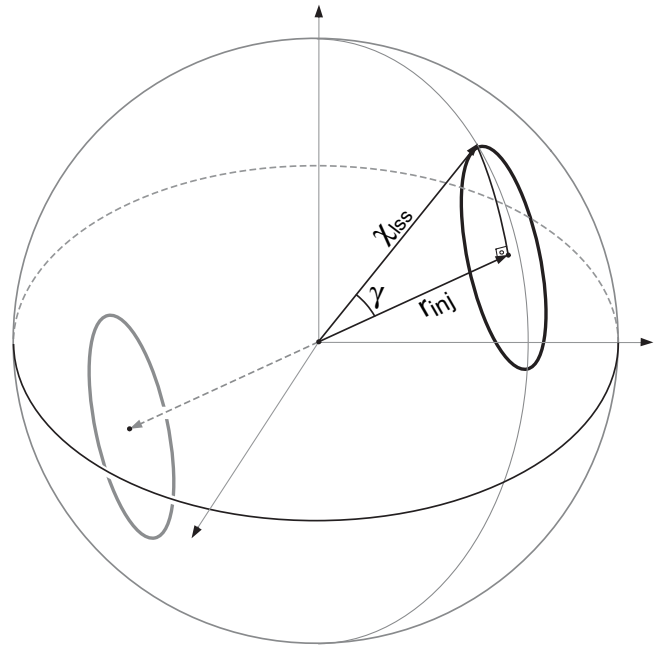

FIG. 1.   A schematic illustration of two antipodal matching circles in the sphere of last scattering. The relation between the angular radius γ and the angular sides r_{inj} and χ_{lss} is given by the following Napier's rule for spherical triangles: $\cos\gamma = \tan r_{inj} \cot\chi_{lss}$ [37].

where d_{lss} is the radius of the LSS, $x = 1 + z$ is an integration variable, H is the Hubble parameter, $\Omega_k = 1 - \Omega_{\text{tot}}$, and $z_{lss} = 1089$ [15]. Equation (7) makes apparent that χ_{lss} depends on the cosmological scenario; moreover, Eq. (6) with χ_{lss} given by Eq. (7) together with Eq. (4) allow us to find a relation between the angular radius γ and the cosmological parameters of the model. Thus, they can be used to set bounds (confidence regions) on these parameters. To quantify this we proceed in the following way. Firstly, for a comparative study we consider a typical angular radius $\gamma = 50°$ estimated in Ref. [13] for the Poincaré dodecahedral space. Secondly, we note that measurements of the radius γ unavoidably involve observational uncertainties, and therefore, in order to set constraints on the density parameters from the detection of cosmic topology, one should take such uncertainties into account. In order to obtain conservative results we consider $\delta\gamma \simeq 6°$, which is the scale below which the circles are blurred in the dodecahedron case [13]. We also analyze the case $\gamma = 11° \pm 1°$, as suggested in Ref. [26].

IV. OBSERVATIONAL CONSTRAINTS FROM SUPERNOVAE DATA AND COSMIC TOPOLOGY

The observations of supernovae measure essentially the apparent magnitude m, which is related to the luminosity distance d_L by

$$m(z) = \mathcal{M} + 5\log_{10}D_L(z), \qquad (8)$$

where

$$D_L(z) \equiv \frac{1}{c} d_L(z), \qquad (9)$$

is the dimensionless luminosity distance and

$$d_L(z) = (1 + z)d_M(z), \qquad (10)$$

with $d_M(z)$ being the comoving distance, given by

$$d_M(z) = \frac{c}{\sqrt{|\Omega_k|}} S_k\left(\sqrt{|\Omega_k|}H_0 \int_0^z \frac{1}{H(z')} dz'\right), \qquad (11)$$

where $S_k(x) = \sin x$ if $\Omega_k < 0$, $S_k(x) = \sinh x$ if $\Omega_k > 0$ and $S_k(x) = x$ if $\Omega_k = 0$. Furthermore,

$$\mathcal{M} = M + 5\log_{10}\left(\frac{c/H_0}{1\text{Mpc}}\right) + 25, \qquad (12)$$

where M is the absolute magnitude which is believed to be constant for all SNe Ia.

For our analysis, we consider the set of SNe Ia data recently compiled by Riess *et al.* [16] known as the *gold* sample. This set contains 143 points from previously published data that were taken from the 230 Tonry *et al.* [29] data along with the 23 points from Barris *et al.* [30]. In order to increase the reliability of the sample, various points where the classification of the supernovae was unclear or the photometry was incomplete were discarded. The *gold* sample contains also 14 points recently discovered using the Hubble Space Telescope consisting altogether of 157 points [16]. The data points in these samples are given in terms of the distance modulus

$$\mu_{\text{obs}}(z) \equiv m(z) - M_{\text{obs}}(z), \qquad (13)$$

and the χ^2 is calculated from

$$\chi^2 = \sum_{i=1}^n \left[\frac{\mu_{\text{obs}}(z_i) - \mathcal{M}' - 5\log_{10}D_{L\text{th}}(z_i; \alpha, A_s)}{\sigma_{\mu_{\text{obs}}}(z_i)}\right]^2, \qquad (14)$$

where $\mathcal{M}' = \mathcal{M} - M_{\text{obs}}$ is a free parameter and $D_{L\text{th}}(z; \alpha, A_s)$ is the theoretical prediction for the dimensionless luminosity distance of a supernova at a particular distance, for the GCG model with parameters α, A_s, which can be computed using the Friedmann expansion rate (see Eq. (4)) combined with Eqs. (9)–(11). The errors $\sigma_{\mu_{\text{obs}}}(z)$ take into account the effects of peculiar motions. We have performed a best-fit analysis with the minimization of the χ^2, Eq. (14), with respect to Ω_k and the GCG model parameters, using a MINUIT [31] based code.

The $\mathcal{D}$ or the $\mathcal{O}$ spatial topology is added to the conventional SNe Ia data analysis as a Gaussian prior on the value of χ_{lss}, which can be easily obtained from an elementary combination of Eqs. (6) and (7) taking into account the ratio H_0/H for the GCG model. In other words, the contribution of the topology to χ^2 is a term of the form $\chi^2_{\text{topology}} = (\chi_{lss}^{\text{Obs}} - \chi_{lss}^{\text{Th}})^2/(\delta\chi_{lss})^2$, where χ_{lss}^{Th} is given by

Eq. (6) and $\delta\chi_{lss}$ is the uncertainty considered in the "circles-in-the-sky" method.

To find the desired confidence regions, we must eliminate the dependence of the χ^2 function on the nuisance parameter $\mathcal{M}'$, and the curvature Ω_k. We first consider the nuisance parameter $\mathcal{M}'$. One way to approach this problem consists in fixing $\mathcal{M}'$ as the value corresponding to the minimum of the χ^2 function. An alternative method consists in marginalizing the likelihood function associated with the χ^2 function over the unwanted parameter, using some probabilistic prior $\pi(\mathcal{M}')$. Using this method, one finds a modified $\tilde{\chi}^2$ function given by

$$\tilde{\chi}^2(\theta) = -2\ln\int\left[\exp\left(-\frac{\chi^2(\theta, \mathcal{M}')}{2}\right)\pi(\mathcal{M}')d\mathcal{M}'\right], \quad (15)$$

where θ stands for the other cosmological parameters.

We marginalize over the nuisance parameter for all cases. We have placed no prior on $\mathcal{M}'$, that is, we considered that all values are equally likely.

As for the curvature, we have used both methods (cf. Figs. 3 and 4). When marginalizing over Ω_k we used the uniform prior that $\Omega_k \in [-0.04, 0.0[$, obtained from WMAP's reported range for the total energy density Ω_{tot} [15]. By using both methods we can have an idea of the sensitivity of the test regarding the curvature parameter. Given that the results are very different for each method (see Figs. 3 and 4), we conclude that the test is quite sensitive to the parameter we are marginalizing over.

In Table I, we summarize the results of our best-fit analysis. Figure 2 shows the results of the SNe Ia analysis alone (no cosmic topology prior). The full and dashed curves represent, respectively, the 68.3% and 95.4% confidence regions in the $\alpha - A_s$ parametric plane. In Fig. 3, we show the results of our joint SNe Ia plus cosmic topology analysis for the case of the $\mathcal{D}$ (top panel) and $\mathcal{O}$ (bottom panel) space topologies, with angular radius $\gamma = 50° \pm 6°$ (left panel) and $\gamma = 11° \pm 1°$ (right panel).

Our results indicate that the combination of SNe Ia data with the detection of either $\mathcal{D}$ or $\mathcal{O}$ spatial topology through the so-called "circles-in-the-sky" method yield some constraints on A_s, which become more important for small values of the angular radius. These constraints are tighter for the $\mathcal{D}$ than for the $\mathcal{O}$ space topology. Indeed,

TABLE I. Best-fit parameters for the GCG model, for a SNe Ia and joint SNe Ia plus cosmic topology analysis, namely, the space topologies $\mathcal{D}$ and $\mathcal{O}$.

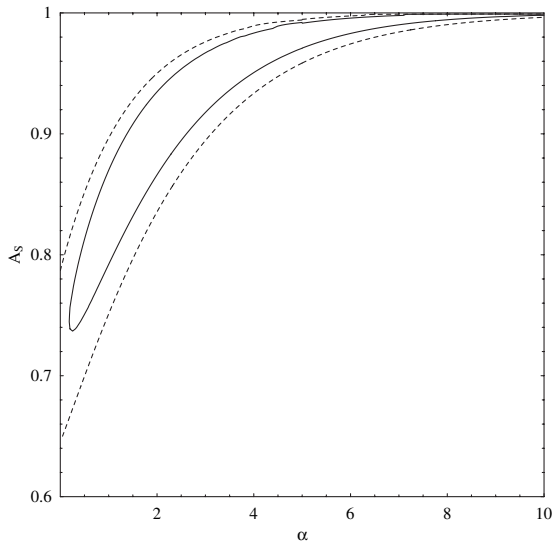| SNe Ia	Topology	γ	A_s	α	Ω_k	χ^2
Gold sample	—	—	0.95	3.07	0.00	174.2
Gold sample	$\mathcal{D}$	50°	0.93	2.58	−0.031	174.3
		11°	0.94	2.83	−0.014	174.3
Gold sample	$\mathcal{O}$	50°	0.89	1.74	−0.040	174.3
		11°	0.94	2.70	−0.023	174.3

FIG. 2. Confidence contours in the $A_s - \alpha$ parameter space for the GCG model, using the SNe Ia *gold* sample. The solid and dashed lines represent the 68% and 95% confidence regions, respectively.

in the former case, we find that $0.754 \lesssim A_s \lesssim 1$ while in the latter $0.74 \lesssim A_s \lesssim 1$, at 68.3% C.L. and for $\gamma = 50°$. For $\gamma = 11°$, bounds are tighter, $0.84 \lesssim A_s \lesssim 1$, for both spatial topologies. These limits are consistent with bounds that can be derived (for the best-fit value of Ω_k) by superimposing the contour curves $\chi_{lss}(A_s, \alpha) = r_{inj}$ for $\mathcal{D}$ and $\mathcal{O}$ on the region of the $\alpha - A_s$ plane allowed by the SNe Ia data [32]. Also notice that the $\mathcal{D}$ space topology is slightly less curved than the $\mathcal{O}$ space topology.

As for the α parameter, we find that it is highly degenerate and, likewise other phenomenological tests, the "circles-in-the-sky" method does not lift this redundancy significantly for the spatial topologies we have analyzed. Actually, so far it has been only through studies of structure formation that a significant dependency on the α parameter has been found (see [33] and references therein). In any case, consistently with the most recent supernova data analysis for the GCG model [17,18], we find that the most likely values for α are greater than one. As for the consistency of our analysis with the one for the ΛCDM model of Ref. [11] we have verified that our results match the ones of that study in the limit $\alpha = 0$.
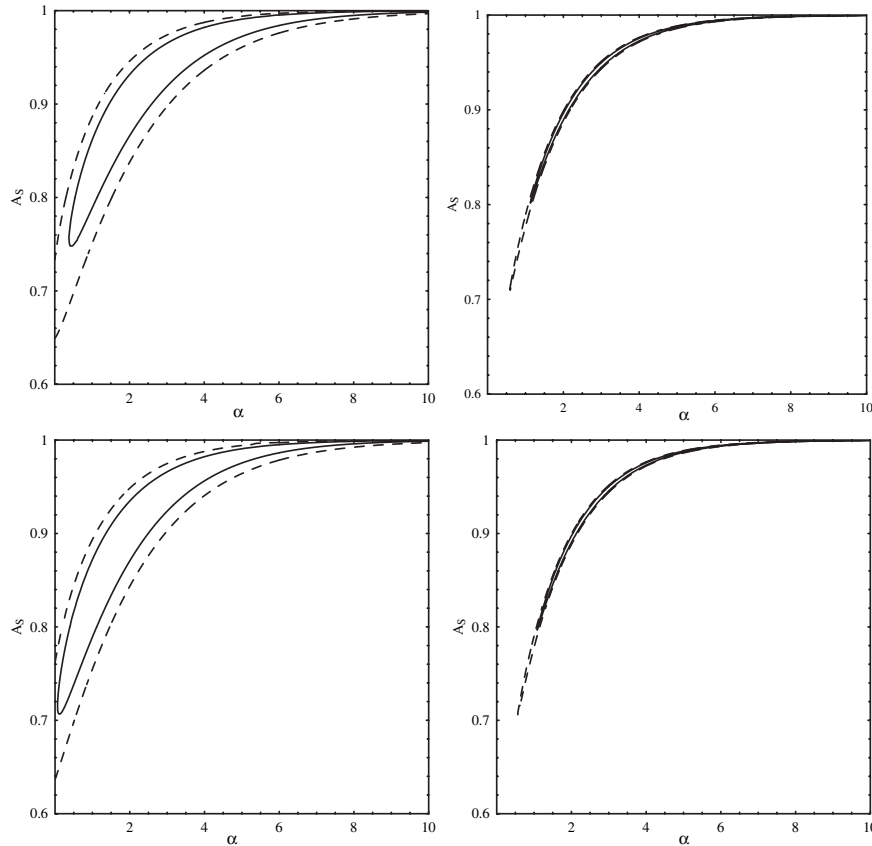

FIG. 3. Confidence contours in the $A_s - \alpha$ parameter space for the GCG model using a joint SNe Ia plus cosmic topology analysis. The top and bottom panels refer to the $\mathcal{D}$ and $\mathcal{O}$ space topology, respectively, with angular radius $\gamma = 50° \pm 6°$ (left panel) and $\gamma = 11° \pm 1°$ (right panel). The solid and dashed lines represent the 68% and 95% confidence regions, respectively. Parameter Ω_k is set at its best-fit value in each case (see Table I).
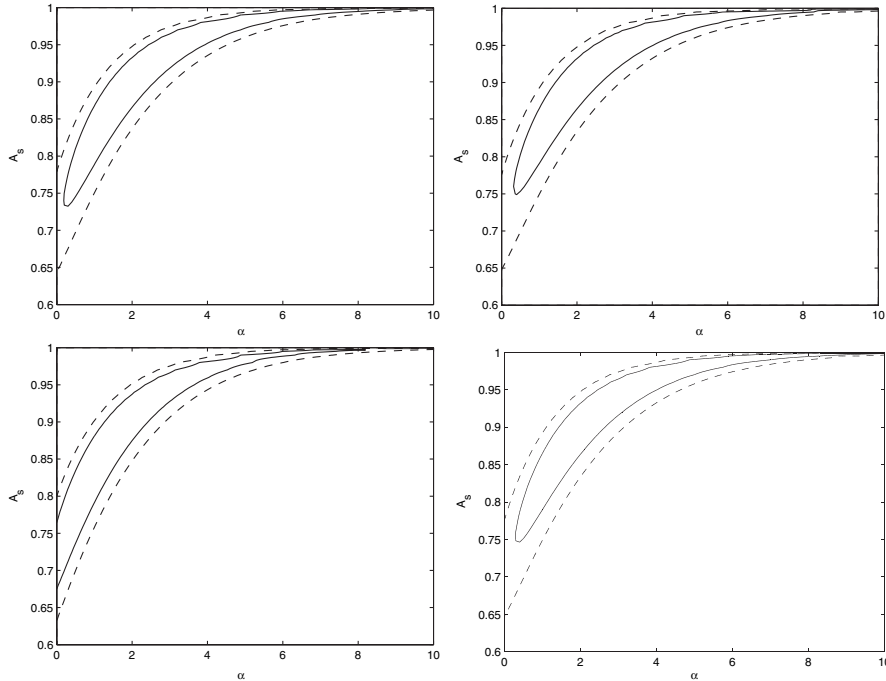
FIG. 4.   As for Fig. 3 but parameter Ω_k has been marginalized over.

Finally, we would like to remark on three important features of our results. First, that the best-fit values are just weakly dependent on the angular radius γ of the circle. Second, that the uncertainty on the value of the radius γ alters predominantly the area corresponding to the confidence regions, without having a significant effect on the best-fit values. Third, there is a topological degeneracy in that the same best fits and confidence regions found for e.g. the $\mathcal{D}$ topology arise from either the $Z_{10} = \mathbb{S}^3/Z_{10}$ or the $\mathcal{D}_5 = \mathbb{S}^3/D_5^*$ globally homogeneous spherical spatial topologies. Similarly, $\mathcal{O}$, $Z_8 = \mathbb{S}^3/Z_8$ and $\mathcal{D}_4 = \mathbb{S}^3/D_4^*$ give rise to identical bounds on the GCG parameters. Here Z_n and D_m^* denotes, respectively, the cyclic and dihedral groups.

V. CONCLUSIONS AND OUTLOOK

The so-called "circles-in-the-sky" method makes apparent that a nontrivial detectable topology of the spatial section of the Universe can be probed for any locally homogeneous and isotropic universe, with no assumption on the cosmological density parameters. In this paper we have shown that the knowledge of $\mathcal{D}$ and $\mathcal{O}$ spatial topologies does provide some additional constraints on the A_s parameter of the GCG model, even though it does not help in lifting the degeneracy on the α parameter.

In any case, our results indicate that the introduction of topological considerations into the analysis of the large scale structure of the Universe is an interesting complementary strategy to constrain and eventually characterize the nature of dark energy and dark matter. In the particular

case of the GCG, the complexity of the model does not allow for obtaining striking constraints on its parameters as is the case for the ΛCDM model. Finally, the question arises whether topology may play a significant role for other dark energy and modified gravity models, an issue we plan to analyze in a future publication.

APPENDIX

Within the framework of FLRW cosmology, the Universe is modeled by a 4-manifold $\mathcal{M}_4$ which is decomposed into $\mathcal{M}_4 = \mathbb{R} \times M_3$, and is endowed with a locally homogeneous and isotropic Robertson–Walker metric, Eq. (2). The spatial section M_3 is usually taken to be one of the following simply-connected spaces: Euclidean $\mathbb{R}^3$ ($k = 0$), spherical $\mathbb{S}^3$ ($k = 1$), or hyperbolic $\mathbb{H}^3$ ($k = -1$) spaces. However, M_3 may equally well be any one of the possible quotient (multiply-connected) manifolds $\mathbb{R}^3/\Gamma$, $\mathbb{S}^3/\Gamma$, and $\mathbb{H}^3/\Gamma$, where Γ is a fixed-point-free discrete group of isometries of the covering space $\mathbb{R}^3$, $\mathbb{S}^3$ and $\mathbb{H}^3$.

The action of Γ tiles the corresponding covering space $\mathbb{R}^3$, $\mathbb{S}^3$ and $\mathbb{H}^3$, into identical cells or domains which are copies of the so-called fundamental polyhedron (FP). A FP plus the face identifications given by the group Γ is a

faithful representation of the quotient manifold M_3. An example of quotient manifold in three dimensions is the flat 3–torus $T^3 = \mathbb{S}^1 \times \mathbb{S}^1 \times \mathbb{S}^1 = \mathbb{R}^3/\Gamma$. The covering space clearly is $\mathbb{R}^3$, and the FP is a cube with opposite faces identified after a translation. This FP tiles the covering space $\mathbb{R}^3$. The group $\Gamma = \mathbb{Z} \times \mathbb{Z} \times \mathbb{Z}$ consists of discrete translations associated with the face identifications.

An important topological feature of the spherical and hyperbolic 3–manifolds M_3 is the so-called injectivity radius r_{inj}, which corresponds to the radius of the smallest sphere that can be inscribed in M_3, which can be formally defined in terms of the length of the smallest closed geodesics ℓ_M by $r_{inj} = \ell_M/2$.

In this work we focus our attention in globally homogeneous spherical manifolds. The multiply-connected spherical 3-manifolds are of the form $M_3 = \mathbb{S}^3/\Gamma$, where Γ is a finite fixed-point-free subgroup of $SO(4)$. The order of Γ gives the number of fundamental polyhedra needed to fulfill the whole covering space $\mathbb{S}^3$. These manifolds were originally classified in Ref. [34] (for a description in the context of cosmic topology see the pioneering article by Ellis [35]). Such a classification consists essentially in the enumeration of all finite groups $\Gamma \subset SO(4)$, and then in grouping the possible manifolds in classes. In a recent paper [36] the classification has been recast in terms of single action, double action, and linked action manifolds. Single action manifolds are globally homogeneous, and then satisfy a topological principle of (global) homogene-

TABLE II. The globally homogeneous spherical manifolds, $M_3 = \mathbb{S}^3/\Gamma$, along with their covering groups, Γ, the order of Γ and the injectivity radius r_{inj}. The cyclic and binary dihedral cases constitute families of manifolds, whose members are given by the different values of the integers n and m.

Name	Covering Group Γ	Order of Γ	r_{inj}
Z_n	Cyclic Z_n	n	π/n
$\mathcal{D}_m$	Binary dihedral D_m^*	$4m$	$\pi/2m$
$\mathcal{T}$	Binary tetrahedral T^*	24	$\pi/6$
$\mathcal{O}$	Binary octahedral O^*	48	$\pi/8$
$\mathcal{D}$	Binary icosahedral I^*	120	$\pi/10$

ity, in the sense that all points in M share the same topological properties. In Table II we list the single action manifolds together with the symbol we use to refer to them, the covering groups Γ and their order as well as the corresponding injectivity radius r_{inj}. We point out that the binary icosahedral group I^* gives rise to the known Poincaré dodecahedral space $\mathcal{D}$, whose FP is a regular spherical dodecahedron, 120 of which tile the 3-sphere into identical cells which are copies of the FP. The FP of the $\mathcal{O}$ space is the truncated cube, 48 of which tile the sphere $\mathbb{S}^3$.

An important point concerning the spherical manifolds is that the injectivity radius r_{inj} expressed in *units of the curvature radius* is a constant (topological invariant) for a given manifold M.

[1] A. Y. Kamenshchik, U. Moschella, and V. Pasquier, Phys. Lett. B **511**, 265 (2001).

[2] N. Bilic, G. B. Tupper, and R. D. Viollier, Phys. Lett. B **535**, 17 (2002).

[3] M. C. Bento, O. Bertolami, and A. A. Sen, Phys. Rev. D **66**, 043507 (2002).

[4] A. G. Riess *et al.* (Supernova Search Team Collaboration), Astron. J. **116**, 1009 (1998); S. Perlmutter *et al.* (Supernova Cosmology Project Collaboration), Astrophys. J. **517**, 565 (1999); C.L. Bennett *et al.*, Astrophys. J. Suppl. Ser. **148**, 1 (2003); D. N. Spergel *et al.*, Astrophys. J. Suppl. Ser. **148**, 175 (2003); M. Tegmark *et al.* (SDSS Collaboration), Phys. Rev. D **69**, 103501 (2004); M. Tegmark *et al.* (SDSS Collaboration), Astrophys. J. **606**, 702 (2004).

[5] See e.g. N. Bahcall, J Ostriker, S. Perlmutter, and P. Steinhardt, Science **284**, 1481 (1999).

[6] M. Lachièze-Rey and J.-P. Luminet, Phys. Rep. **254**, 135 (1995); G. D. Starkman, Class. Quant. Grav. **15**, 2529 (1998); J. Levin, Phys. Rep. **365**, 251 (2002); M. J. Rebouças and G.I. Gomero, Braz. J. Phys. **34**, 1358 (2004); M. J. Rebouças, AIP Conf. Proc. **782**, 201 (2005).

[7] R. Lehoucq, M. Lachièze-Rey, and J.-P Luminet, Astron. Astrophys. **313**, 339 (1996); B. F. Roukema, Class. Quant.

Grav. **15**, 2645 (1998); R. Lehoucq, J.-P Luminet, and J.-P. Uzan, Astron. Astrophys. **344**, 735 (1999); H. V. Fagundes and E. Gausmann, Phys. Lett. A **238**, 235 (1998); J.-P. Uzan, R. Lehoucq, and J.-P. Luminet, Astron. Astrophys. **351**, 766 (1999); G. I. Gomero, M. J. Rebouças, and A. F. F. Teixeira, Int. J. Mod. Phys. D **9**, 687 (2000); R. Lehoucq, J.-P. Uzan, and J.-P Luminet, Astron. Astrophys. **363**, 1 (2000); G. I. Gomero, M. J. Rebouças, and A. F. F. Teixeira, Phys. Lett. A **275**, 355 (2000); G. I. Gomero, M. J. Rebouças, and A. F. F. Teixeira, Class. Quant. Grav. **18**, 1885 (2001); G. I. Gomero, A. F. F. Teixeira, M. J. Rebouças, and A. Bernui, Int. J. Mod. Phys. D **11**, 869 (2002); A. Marecki, B. Roukema, and S. Bajtlik, Astron. Astrophys. **435**, 427 (2005).

[8] G. I. Gomero, M. J. Rebouças, and R. Tavakol, Class. Quant. Grav. **18**, 4461 (2001); G. I. Gomero, M. J. Rebouças, and R. Tavakol, Class. Quant. Grav. **18**, L145 (2001); G. I. Gomero, M. J. Rebouças, and R. Tavakol, Int. J. Mod. Phys. A **17**, 4261 (2002); J. R. Weeks, R. Lehoucq, and J.-P. Uzan, Class. Quant. Grav. **20**, 1529 (2003); J. R. Weeks, Mod. Phys. Lett. A **18**, 2099 (2003); G. I. Gomero and M. J. Rebouças, Phys. Lett. A **311**, 319 (2003); B. Mota, M. J. Rebouças, and R. Tavakol, Class. Quant. Grav. **20**, 4837 (2003).

[9] N. J. Cornish, D. Spergel, and G. D. Starkman, Class. Quant. Grav. **15**, 2657 (1998).

[10] M. O. Calvão, G. I. Gomero, B. Mota, and M. J. Rebouças, Class. Quant. Grav. **22**, 1991 (2005).

[11] M. J. Rebouças, J. S. Alcaniz, B. Mota, and M. Makler, astro-ph/0511007.

[12] J.-P. Luminet, J. Weeks, A. Riazuelo, R. Lehoucq, and J.-P. Uzan, Nature (London) **425**, 593 (2003).

[13] R. Aurich, S. Lustig, and F. Steiner, Class. Quant. Grav. **22**, 2061 (2005).

[14] R. Aurich, S. Lustig, and F. Steiner, Class. Quant. Grav. **22**, 3443 (2005).

[15] D. N. Spergel *et al.*, Astrophys. J. Suppl. Ser. **148**, 175 (2003).

[16] A. G. Riess *et al.* (Supernova Search Team Collaboration), Astrophys. J. **607**, 665 (2004).

[17] O. Bertolami, A. A. Sen, S. Sen, and P. T. Silva, Mon. Not. R. Astron. Soc. **353**, 329 (2004).

[18] M. C. Bento, O. Bertolami, N. M. C. Santos, and A. A. Sen, Phys. Rev. D **71**, 063501 (2005).

[19] M. C. Bento, O. Bertolami, and A. A. Sen, Phys. Rev. D **67**, 063003 (2003); Phys. Lett. B **575**, 172 (2003); Gen. Relativ. Gravit. **35**, 2063 (2003).

[20] D. Carturan and F. Finelli, Phys. Rev. D **68**, 103501 (2003); Amendola, F. Finelli, C. Burigana, and D. Carturan, J. Cosmol. Astropart. Phys. 07 (2003) 005.

[21] J. C. Fabris, S. B. V. Gonçalves, and P. E. de Souza, astro-ph/0207430; A. Dev, J. S. Alcaniz, and D. Jain, Phys. Rev. D **67**, 023515 (2003); V. Gorini, A. Kamenshchik, and U. Moschella, Phys. Rev. D **67**, 063509 (2003); M. Makler,

S. Q. de Oliveira, and I. Waga, Phys. Lett. B **555**, 1 (2003); J. S. Alcaniz, D. Jain, and A. Dev, Phys. Rev. D **67**, 043514 (2003).

[22] P. T. Silva and O. Bertolami, Astrophys. J. **599**, 829 (2003).

[23] A. Dev, D. Jain, D. D. Upadhyaya, and J. S. Alcaniz, Astron. Astrophys. **417**, 847(2004).

[24] O. Bertolami and P. T. Silva, Mon. Not. R. Astron. Soc. **365**, 1149 (2006).

[25] N. J. Cornish, D. N. Spergel, G. D. Starkman, and E. Komatsu, Phys. Rev. Lett. **92**, 201302 (2004).

[26] B. F. Roukema *et al.*, Astron. Astrophys. **423**, 821 (2004).

[27] J. Gundermann, astro-ph/0503014.

[28] R. Aurich, S. Lustig, and F. Steiner, astro-ph/0510847.

[29] J. L. Tonry *et al.* (Supernova Search Team Collaboration), Astrophys. J. **594**, 1 (2003).

[30] B. J. Barris *et al.*, Astrophys. J. **602**, 571 (2004).

[31] http://cernlib.web.cern.ch/cernlib/download/2004_source/tar/minuit32_src.tar.gz.

[32] M. Makler, B. Mota, and M. J. Rebouças, astro-ph/0507116.

[33] M. C. Bento, O. Bertolami, and A. A. Sen, Phys. Rev. D **70**, 083519 (2004).

[34] W. Threlfall and H. Seifert, Math. Ann. **104**, 543 (1932).

[35] G. F. R. Ellis, Gen. Relativ. Gravit. **2**, 7 (1971).

[36] E. Gausmann, R. Lehoucq, J.-P. Luminet, J.-P. Uzan, and J. Weeks, Class. Quant. Grav. **18**, 5155 (2001).

[37] H. S. M. Coxeter, *Non-Euclidean Geometry* (University of Toronto Press, Toronto, 1965) 5th ed.